arXiv:astro-ph/0306232v1 11 Jun 2003

The distance and radius of the neutron star PSR B0656+14

Walter F. Brisken,[1] S. E. Thorsett,[2] A. Golden,[3] & W. M. Goss[1]

ABSTRACT

We present the result of astrometric observations of the radio pulsar PSR B0656+14, made using the Very Long Baseline Array. The parallax of the pulsar is $\pi = 3.47 \pm 0.36$ mas, yielding a distance 288^{+33}_{-27} pc. This independent distance estimate has been used to constrain existing models of thermal x-ray emission from the neutron star's photosphere. Simple blackbody fits to the x-ray data formally yield a neutron star radius $R_\infty \sim 7 - 8.5$ km. With more realistic fits to a magnetized hydrogen atmosphere, any radius between ~ 13 and ~ 20 km is allowed.

Subject headings: stars: neutron, equation of state—pulsars: individual (PSR B0656+14)—astrometry

1. Introduction

The cooling of neutron stars offers a unique diagnostic of the physics of the interior. Because the emergent spectrum is nearly blackbody, the observed flux can be modeled to estimate the temperature, the intervening column of absorbing material, and the ratio of radius to distance. Astrometric measurement of the distance then allows an estimation of the photospheric radius, which is sensitively dependent on the high density equation of state.

PSR B0656+14 is a middle-aged ($\sim 10^5$ yr old) pulsar, with a spectrum dominated at ultraviolet and soft-X-ray wavelengths by a $\sim 10^6$ K blackbody component, as expected in standard cooling models. Distance estimates obtained from measurements of radio dispersion in the ionized material between Earth and the pulsar have led to a large estimated stellar radius, > 20 km. Here we show that the parallax of PSR B0656+14, determined using very long baseline interferometry, leads to a factor three reduction in the estimated pulsar distance. We place this result in the context of existing thermal models for the neutron star.

[1]National Radio Astronomy Observatory, PO Box O, Socorro, NM 87801;

[2]Department of Astronomy and Astrophysics, University of California, Santa Cruz, CA 95064

[3]National University of Ireland, Newcastle Road, Galway, Republic of Ireland

2. VLBA Observations & Astrometric Analysis

For many years, pulsar parallax measurements have been just at or beyond experimental limits. The situation has greatly improved with the increased sensitivity available using the NRAO[4] Very Long Baseline Array (VLBA), together with new phase-referencing techniques for measuring and eliminating ionospheric distortion and the ability to gate the VLBA correlator to accept data only during intervals when the pulsar is "on." In the last three years, parallaxes (and distances) to ten pulsars have been measured with the VLBA (Brisken et al. 2002; Chatterjee et al. 2001).

PSR B0656+14 has a 1.4 GHz flux density of 3.6 mJy, which is too weak to use the ionosphere calibration technique described by Brisken et al. (2002). Instead, the in-beam calibration technique used by Chatterjee et al. (2001) was applied. Very Large Array (VLA) observations were made in the A-configuration at 1.4 GHz to search for potential in-beam calibrators. Three candidates were followed up at 8.4 and 15 GHz to test for compactness. Fortunately one of them, 0658+1410, was compact and bright enough for use as an in-beam calibrator. See Table 1 for a list of calibrators used, their coordinates, and their flux densities.

[4]The National Radio Astronomy Observatory is a facility of the National Science Foundation operated under cooperative agreement by Associated Universities, Inc.

Five observations of PSR B0656+14, each five hours long, were made over 1.3 yrs with the VLBA. A 32 MHz band centered at 1.6675 GHz was used, resulting in a beam size of 15×6 mas. Each observation consisted of sixty 2 minute scans on the field containing the pulsar and in-beam calibrator, each bracketted by observations of J0637+1458, and two 5 minute scans on 3C147 for bandpass calibration. The target field was correlated twice. The first correlation placed the in-beam calibrator at the phase center. The second put the pulsar at the phase center and used the pulsar gate to improve the signal-to-noise.

Considerable effort went into ensuring that each observation was reduced identically. Analysis used the standard AIPS package. After editing the data to remove radio-frequency interference, data from all five epochs were combined to make a single model for each calibrator source using standard techniques. After initial amplitude and bandpass calibration, GPS-based ionosphere calibrations were applied with the task TECOR. J0637+1458 was then fringe fitted (with the model) to determine the delays and rates and to perform a first-order phase calibration, which was followed by phase-and-amplitude self-calibration. Calibration derived from J0637+1458 was interpolated in time and applied to 0658+1410. This source was self-calibrated for phases only, again with a model. The calibrations from both J0637+1458 and 0658+1410 were applied to the pulsar, images were produced, and image-plane Gaussian fitting performed to determine the pulsar position.

Uncertainties are dominated by systematic effects, mainly due to atmospheric and ionospheric refraction. To estimate the size of these effects, imaging was repeated at each epoch with subsets of the data. The measured position varied most with varying time cuts. The scatter in position when varying the time ranges was used to assign error bars. Final single-epoch position uncertainties were 0.8 mas and 0.4 mas in right ascension and declination respectively. The position of B0656+14 at each epoch is shown in Table 2. Note that the absolute positions are accurate only to about 10 mas due to the uncertainty in the true position of the calibrator 0658+1410.

The five measured positions were used to simultaneously fit the parallax, π, proper motion ($\mu_\alpha \cos(\delta)$ and μ_δ), and position of PSR B0656+14. These values and the derived distance, transverse velocity, $v_\perp$, and line-of-sight column density of electrons, n_e are shown in Table 3. Figure 1 shows the parallax fit to the data points. In this plot, the proper motion has been removed from the data to allow the subtle parallax to be seen.

The proper motion measured here differs from that measured by Thompson and Córdova (1994), $\mu_\alpha \cos\delta = 64 \pm 11$ and $\mu_\delta = -28 \pm 4$ mas/yr, by more than 6σ. It is in excellent agreement with the *HST*-derived value, $\mu_\alpha \cos\delta = 42.7 \pm 2$ and $\mu_\delta = -2.1 \pm 3$ mas/yr (Mignani, De Luca, & Caraveo 2000), though somewhat more precise.

3. Discussion

3.1. Implications for Galactic electron density model

The distance determined from the pulsar dispersion measure (DM) using the Galactic electron distribution model of Taylor and Cordes (1993) is 760±190 pc. Using the electron distribution model of Cordes and Lazio (2002) yields 669 ± 73 pc. Both values are substantially greater than the parallax distance, 288^{+33}_{-27} pc. The discrepancy is not entirely surprising—the galactic electron density is poorly sampled at this (l, b) due to a lack of calibration sources near the 201° galactic latitude of PSR B0656+14 (Anderson et al. 1993). Furthermore, the nearest calibration source for the Taylor & Cordes model, PSR B0823+26 at $l = 197°$, is known to have a DM derived distance some 3 times its measured parallax (Gwinn et al. 1986). Nevertheless, the high mean electron density along this path, $n_e = 0.049$ cm^{-3}, is a reminder that dispersion distances are particularly uncertain in the Solar neighborhood, where lines of sight do not average over many independent regions.

3.2. Implications for thermal modeling and the stellar radius

PSR B0656+14 has been extensively studied at optical (Shearer et al. 1997; Kurt et al. 1998; Koptsevich et al. 2001), ultraviolet (Pavlov, Stringfellow, & Córdova 1996; Pavlov, Welty, & Córdova 1997; Edelstein et al. 2000), x-ray (Córdova et al. 1989; Finley, Ögelman, & Kiziloğlu 1992; Anderson et al. 1993; Greiveldinger et al. 1996; Mineo et al. 2002; Marshall & Schulz 2002;

Pavlov et al. 2002), and gamma-ray (Ramanamurthy et al. 1996) energies.

A simple model that adequately accounts for observations from the optical through the x-ray bands includes a power law component, identified with non-thermal emission from the active magnetosphere, and two blackbody components: a harder component identified with the heated polar caps, and a softer component identified with emission from the entire photosphere. In general, model fits agree very well. For example, a model based on the *EUVE, ROSAT,* and *ASCA* data (Koptsevich et al. 2001) gives $T_\infty = 8.4 \pm 0.3 \times 10^5$ K for the temperature of the soft component, while an independent model based on *Chandra* observations (Marshall & Schulz 2002) gives $T_\infty = 8.0 \pm 0.3 \times 10^5$ K, where T_∞ is the gravitationally redshifted temperature measured by a distant observer: $T_\infty = T(1 - 2GM/Rc^2)^{1/2}$. For our distance of 288 pc, the resulting estimates for the radius of the neutron star, $R_\infty = R(1 - 2GM/Rc^2)^{-1/2}$ are 7.8 and 8.5 km, respectively. Including the optical/UV data and forcing a single power-law slope for the non-thermal component across more than four orders of magnitude in energy, Pavlov et al. (2002) find a slightly smaller radius, 6.9 km at 288 pc. Estimates for the radius of the hot polar cap vary from 0.5 to 0.64 km at that distance.

A blackbody radius as small as $R_\infty = 8$ km would pose serious challenges to standard neutron star models (e.g., Heiselberg & Pandharipande 2000), though it would be acceptable for a low mass strange star (Alcock, Fahri, & Olinto 1986). However, a more likely explanation for this anomalous result is failure of the simple black-body modeling.[5]

In general, realistic atmosphere models tend to shift flux into high energy tails that result in overestimation of the effective temperature and hence underestimation of the stellar radius (see Romani 1987 and Shibanov et al. 1992 for early work on non-magnetic and magnetic atmospheres, respectively, and Zavlin & Pavlov 2002 for a recent review). The largest radii are found with non-magnetic hydrogen or helium atmospheres, while strong magnetic fields suppress the high energy tails and produce intermediate temperature and radius estimates. Our blackbody model radius should therefore most properly be treated as a lower limit to the neutron star radius.

For PSR B0656+14, fits to unmagnetized hydrogen atmospheres (e.g., Marshall & Schulz 2002) produce very large radius estimates: ~ 156 km at our measured distance. This can be regarded as an (unconstraining) upper limit to the radius.

Magnetized atmospheres produce much more reasonable results. Using just the *ROSAT* data, the magnetic hydrogen models of Shibunov et al. (1993), and a canonical neutron star radius of $R_\infty = 13$ km, Anderson et al. (1993) estimated the pulsar distance to be 280^{+60}_{-50} pc, in remarkable agreement with our measurement. Scaling from model fits done for the Geminga pulsar, Marshall & Schulz (2002) estimate that the using a magnetized hydrogen atmosphere will increase the radius by a factor 2.3 over a blackbody estimate, resulting in corrected radius estimates of 15.9, 17.9, and 19.7 km for the Pavlov et al. (2002), Koptsevich et al. (2001), and Marshall & Schulz (2002) model fits, respectively. We conclude that within the model uncertainties, any radius R_∞ between ~ 13 and ~ 20 km is allowed.

3.3. The next steps

A promising observational approach is to complement the high-energy observations with improved constraints on the flux in the optical and ultraviolet bands. Anderson et al. (1993) found that the blackbody and magnetized hydrogen atmosphere models that each fit the *ROSAT* data have significantly different predictions in the optical bands: for example, $B \approx 28.7$ and $B \approx 27.8$, respectively.

Analysis of the combined integrated photometric data indicate that the spectral energy distribution is predominantly thermal in the ultraviolet, then flattens out and asymptotically approaches a power-law-like form towards the infrared (Koptsevich et al. 2001). The photometry is well fit by a Rayleigh-Jeans plus synchrotron-like power-

[5]There has also been some concern that flux from an apparent pulsar wind nebula that has been barely resolved by *Chandra* might contaminate the x-ray spectra (Pavlov et al. 2002). Because the estimated luminosity is less than 4% of the bolometric luminosity of the soft thermal component, any systematic effect on the radius estimation is likely to be small, but larger errors might be introduced to the polar cap radius.

law model—the former agreeing to first order with the X-ray extrapolations. The power-law, with a best-fit index ~ 1.5, is similar to that observed at hard-x-ray and gamma-ray energies.

In the ultraviolet, comparisons with model predictions are challenging because of the uncertain reddening. In the optical, the challenge has been to detect the thermal contribution beneath the larger non-thermal power-law. The observed B magnitude is $24.85^{+0.19}_{-0.16}$ (Kurt et al. 1998), more than an order of magnitude above the expected thermal contribution.

Of considerable interest, then, has been the detection of optical pulsations. Shearer et al. (1997) reported pulsations based on B-band observations with a 2-d counting MAMA camera, and Kern (2002) detected pulsations in the $\sim V$ band using a phase-binning CCD system. In addition to confirming the magnetospheric origin of the optical radiation, these observations raise the possibility of measuring and removing the non-thermal component. While there are clear differences in the light curve morphologies, both datasets are consistent with the radiation being 100% pulsed. At this time, only upper limits can be placed on any unpulsed thermal emission: in B, the limit is $B \leq 26.8$. This is within a factor ~ 3 of the predicted value. Of considerable interest would be extending these observations to U band, where the nonthermal flux will be smaller and the predicted thermal flux is a factor four higher.

These observations will be challenging, as will continued improvement in the magnetic atmosphere modeling. But both observations and theory have seen remarkable improvement over the last decade, even when the ultimate limit was the very uncertain pulsar distance. Now the distance to PSR B0656+14 is known to 10%, comparable to the typical uncertainty of individual spectral model fits, and somewhat below the systematic uncertainties in the atmospheric fitting. There is no reason that continued radio observations shouldn't continue to improve the parallax limit: precision a factor five better has now been achieved for PSR B0950+08. Thus there is every reason to believe that PSR B0656+14 will continue to develop into a fascinating astrophysical laboratory for nuclear physics.

We wish to thank Andrew Lyne for providing us with the pulsar ephemeris that allowed us to gate the VLBA correlator. S.E.T. is supported by the NSF under grant AST-0098343. A.G. is supported by Enterprise Ireland under grant SC/2001/322.

REFERENCES

Alcock, C., Farhi, E., & Olinto, A. 1986, ApJ, 310, 261

Anderson, S. B., Córdova, F. A., Pavlov, G. G., Robinson, C. R., & Thompson, R. J., Jr. 1993, ApJ, 414, 867

Brisken, W. F., Benson, J. M., Goss, W. M., & Thorsett, S. E. 2002, ApJ, 571, 906

Chatterjee, S., Cordes, J. M., Goss, W. M., Fomalont, E. B., Beasley, A. J., Lazio, T. J. W., & Arzoumanian, Z. 2001, ApJ, 550, 287

Cordes, J. M. & Lazio, T. J. W., 2002, submitted (astro-ph/0207156)

Córdova, F. A., Middleditch, J., Hjellming, R. M., & Mason, K. O. 1989, ApJ, 345, 451

Edelstein, J., Seon, K.-I., Golden, A., & Min, K.-W. 2000, ApJ, 539, 902

Finley, J. P., Ögelman, H., & Kiziloğlu, Ü. 1992, ApJ, 394, L21

Greiveldinger, C., et al. 1996, ApJ, 465, L35

Gwinn, C. R., Taylor, J. H., Weisberg, J. M., & Rawley, L.A. 1986, AJ, 91, 338

Heiselberg, H. & Pandharipande, V. 2000, Ann. Rev. Nuc. Part. Sci., 50, 481

Kern, B., PhD Thesis, California Institute of Technology, May 2002

Koptsevich, A. B., Pavlov, G. G., Zharikov, S. V. et al., 2001, A&A, 370, 1004

Kurt, V. G., Sokolov, V. V., Zharikov, S. V., Pavlov, G. G., & Komberg, B. V., 1998, A&A, 333, 547

Marshall, H. L. & Schultz, N. S., 2002, ApJ, 574, 377

Mignani, R. P., De Luca, A., & Caraveo, P. A. 2000, ApJ, 543, 318

Mineo, T., Massaro, E., Cusumano, G., & Becker, W. 2002, A&A, 392, 181

Pavlov, G. G., Zavlin, V. E., & Sanwal, D. 2002, in Neutron Stars, Pulsars, and Supernova Remnants, ed. W. Becker, H. Lesch, & J. Trümper (Garching bei München: Max-Planck-Institut für extraterrestrische Physik), 273.

Pavlov, G. G., Stringfellow, G. S., & Córdova, 1996, ApJ, 467, 370.

Pavlov, G. G., Welty, A. D., & Córdova, F. A. 1997, ApJ, 489, L75

Ramanamurthy, P. V., Fichtel, C. E., Kniffen, D. A., Sreekumar, P., & Thompson, D. J. 1996, ApJ, 458, 755

Romani, R. W. 1987, ApJ, 313, 718

Shearer, A. et al. 1997, ApJ, 478, L181

Shibunov, Yu. A., Zavlin, V. E., Pavlov, G. G., & Ventura, J. 1992, A&A, 266, 313

Shibunov, Yu. A., Zavlin, V. E., Pavlov, G. G., Ventura, J., & Potehkin, A. Yu. 1993, in Isolated Pulsars, ed. K. A. Van Riper, R. I. Epstein, & C. Ho (Cambridge, UK: Cambridge Univ. Press), 174

Taylor, J. H., & Cordes, J. M. 1993, ApJ, 411, 674

Thompson, R. J. & Córdova, F. A. 1994, ApJ, 434, 54

Zavlin, V. E. & Pavlov, G. G. 2002, in Neutron Stars, Pulsars, and Supernova Remnants, ed. W. Becker, H. Lesch, & J. Trümper (Garching bei München: Max-Planck-Institut für extraterrestrische Physik), 263

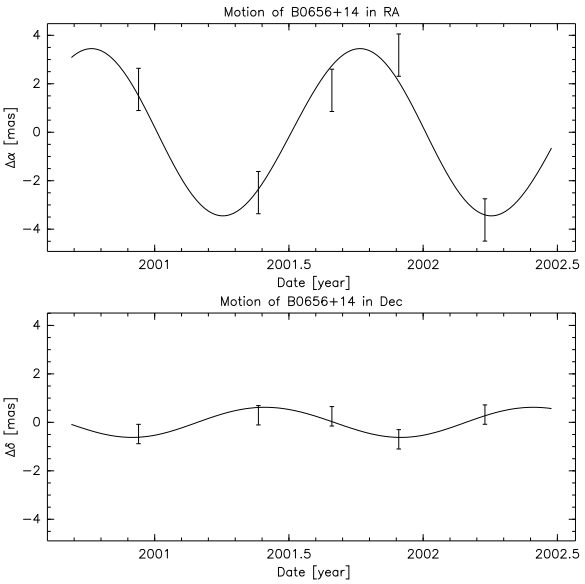

Fig. 1.— The parallax fit to five measured positions of B0656+14. The proper motion was removed from the data and model.

This 2-column preprint was prepared with the AAS LaTeX macros v5.0.

Table 1
Calibrator sources

Object	$\alpha_{\rm J2000}$	$\delta_{\rm J2000}$	Peak S_{1667}[†] (mJy/beam)	Int. S_{1667}[†] (mJy)	Remarks
3C147	$05^h42^m36^s.1379$	$49°51'07''.234$	1493	2998	Bandpass calibrator
J0637+1458	$06^h37^m51^s.0523$	$14°58'57''.278$	234	250	Phase calibrator
0658+1410	$06^h58^m46^s.285$	$14°10'37''.83$	33	38	In-beam calibrator

[†]Peak and integrated flux densities are averaged over the 1651.5 to 1683.5 MHz observed band.

Table 2
B0656+14 position measurements

Date	$\alpha_{\rm J2000}$	$\delta_{\rm J2000}$
2000.940	$06^h59^m48^s.15018$	$14°14'21''.1576$
2001.386	$06^h59^m48^s.15124$	$14°14'21''.1573$
2001.660	$06^h59^m48^s.15236$	$14°14'21''.1566$
2001.909	$06^h59^m48^s.15322$	$14°14'21''.1551$
2002.230	$06^h59^m48^s.15372$	$14°14'21''.1553$

TABLE 3
DERIVED PARAMETERS FOR B0656+14

Parameter	Value[†]
$\alpha_{\rm J2000}$[‡]	$06^h59^m48^s.1472$
$\delta_{\rm J2000}$[‡]	$14°14'21''.160$
$\mu_\alpha \cos(\delta)$	44.07 ± 0.63 mas yr^{-1}
μ_δ	-2.40 ± 0.29 mas yr^{-1}
π	3.47 ± 0.36 mas
Distance	288^{+33}_{-27} pc
$v_\perp$	60^{+7}_{-6} km s^{-1}
$n_{\rm e}$	0.048 ± 0.005 cm^{-3}

[†]Uncertainties are 68% confidence intervals.

[‡]The pulsar position is relative to the frame defined by 0658+1410. The uncertainty in the coordinates of 0658+1410 dominate the total uncertainty of the pulsar's absolute position and are estimated to be about 10 mas.